Integrated and Flexible High Temperature Ultrasonic Transducers

Makiko Kobayashi and Cheng-Kuei Jen

Industrial Materials Institute, National Research Council of Canada, Boucherville, Quebec, Canada J4B 6Y4

ABSTRACT:

Thick (> 40µm) ceramic films as piezoelectric ultrasonic transducers (UTs) have been successfully deposited on metallic and graphite/epoxy composite substrates by a spray technique. The characteristics of these UTs are that they (1) can be integrated directly onto the desired planar or curved substrates; (2) may not need couplant; (3) can operate in the transmission and pulse/echo modes with a signal to noise ratio more than 30 dB at 2-15 MHz; (4) can operate up to more than 400°C; (5) can be made flexible and (6) can be made as UT array. The capability using these UT for longitudinal and shear generation and receiving probe is demonstrated. Such films have been also deposited onto thin stainless steel membranes to form the flexible UT array for high temperature applications.

1. INTRODUCTION

Ultrasonic methods employing piezoelectric ultrasonic transducers (UTs) have been widely used to perform NDT on large metallic and composite structures such as airplane frames, pipes, engines, pressure vessels, etc because of the subsurface inspection capability, simplicity and cost-effectiveness [1-4]. Many of these NDT applications [5-9] plus the need for real-time in-line noninvasive diagnostics of industrial materials processes [10,11] demand high temperature (HT) piezoelectric UTs. The limitations of the current HTUTs are (1) the requirement of couplant, (2) complicated to be used for curved surfaces, (3) difficult to be used for pulse-echo mode and (4) difficult to be used as flexible and array UTs. In this investigation, we are reporting the use of thick film (>40 µm) piezoelectric ceramic UTs as integrated and flexible UTs onto metals and graphite/epoxy composites with flat and curved surfaces at temperatures up to 400°C.

It is understood that for NDT and characterization of material shear (S) waves may be advantageous over longitudinal (L) wave because liquid and gas medium do not support S waves [1,12,13]. In addition, for the evaluation of material properties sometimes it is important to know that shear modulus and visco-elastic properties in which S waves properties are a requisite. Furthermore, a probe setup that can be used to generate and receive both L and S waves at the same sensor location would be also of interest. In the past special crystal cut, for example, 10° rotated Y-cut lithium niobate and tilted C-axis zinc oxide thin films were reported to generate and receive both L and S waves simultaneously [14]. In this study, methods are presented to achieve HT integrated ultrasonic S wave transducer and also provide a means to excite and receive both L and S waves at elevated temperatures.

2. FABRICATION AND CHARACTERIZATION

Thick piezoelectric ceramic films made by the technologies of jet printing, screen printing, dipping, tape casting, hydrothermal method, etc. were reported. Here a

composite spray technique is used because of its simplicity and capability to coat films on various metallic substrates of different shapes. Sol-gel fabricated thick films were firstly reported at Queen's [15], however; the aims were not for HT NDT applications and the fabrication techniques did not consider the large size substrates such as metallic pipes and molds. In this study, the piezoelectric lead zirconate titanate (PZT) or bismuth titanate (BIT) powders were first purchased with an averaged dimension of 2-200 µm and dispersed into PZT solution by ball milling method to achieve the gel. The final dimension of the PZT or BIT powder is estimated to be less than 1µm. PZT was selected due to its high piezoelectric constant, high dielectric constant and around 350°C Curie temperature. BIT was chosen because of its high Curie temperature, 675°C and reasonable piezoelectric strength. A handheld air gun [14] was then used to spray the sol-gel composite directly onto samples large or small even with curved surfaces. With this technique, such films designated as PZT/PZT or BIT/PZT can easily be produced at desired locations through a shadow mask made of even paperboard. After spray coating, a furnace, a heat gun or a gas burner such as handheld propane bottle with nozzle are used to perform drying and firing, respectively with the optimal time duration. The advantage of the heat gun or gas burner is that the film can be made at the desired NDT site without the need of the furnace. Multiple layers were made in order to reach the desired thickness. The 40 – 120 µm thick films, to provide the desired centre frequency in the range of 2 – 30 MHz, were produced. This frequency range is commonly preferred for NDT of metals and industrial material process monitoring [10,11] because of its sufficient ranging resolution and acceptable ultrasonic attenuation in metals and polymers.

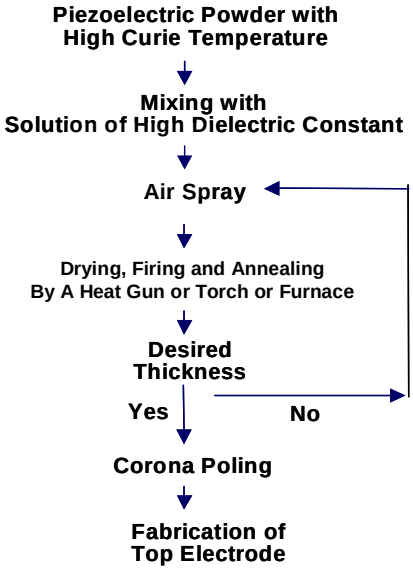

Fig.1. Flow chart of the fabrication process of piezoelectric thick film UT.

The films were then electrically poled using the corona discharging technique to achieve the piezoelectricity and the temperature of the substrate at the film location was kept between 120°C and 350°C. During poling a high positive voltage supplied from a high voltage DC power supply was fed into a needle which was located several

centimeters above the film coated on the metal substrate which served as the ground electrode. The distance and voltage were optimized for different film thicknesses and geometries. The poling time was about 10 minutes. The corona poling method was chosen because it could pole the thick piezoelectric ceramic film of a large area and on curved surfaces with ease. Afterwards the top electrode was made by manually written by silver or platinum paste. The platinum paste has been tested and its operating temperature could be above 440°C. Electrical connections can be then made between the ultrasonic pulser-receiver and the two electrodes for ultrasonic measurements. Figure 1 presents the flow chart of the fabrication process of the thick film UTs described above.

The measured relative dielectric constant of the PZT/PZT film was around 320 and that for BIT/PZT 80. The d_{33} measured by an optical interferometer is 30 (10^{-12} m/V) for PZT/PZT and 11 (10^{-12} m/V) for BIT/BIT. The electromechanical coupling constant measured was 0.2 for PZT/PZT and that for BIT/PZT is a weaker.

3. INTEGRATED LONGITUDINAL WAVE UTs

3.1 On Metal Substrate

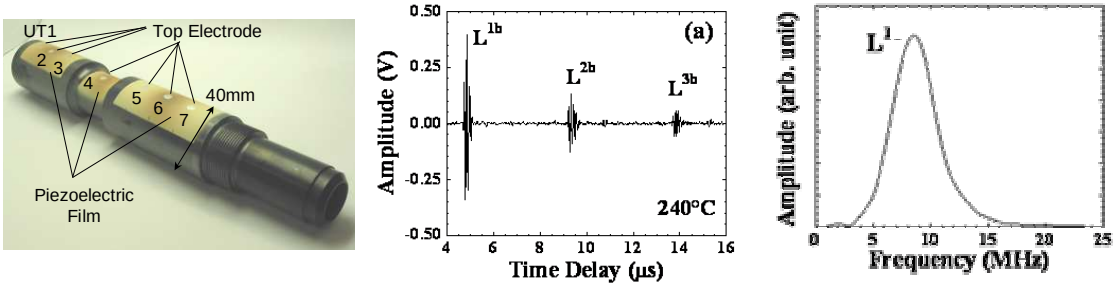

(a) (b) (c)

Fig.2. (a) Seven UTs fabricated directly onto a steel barrel (tube) of a micromolding machine, ultrasonic performance of UT6 in (b) time and (c) in frequency domain at 240°C.

Figure 2 shows seven L wave UTs (UT1-7) fabricated directly onto the external surface of the cylindrical steel barrel of a micromolding machine [11]. The objective was to perform real-time diagnostics of micro-molding process using these UT along the barrel. The length of the barrel was 265mm, the internal diameter was 14mm, and the external diameter at the areas of UT1-3, 5-7 and at that of UT4 were 40mm and 30mm, respectively. As shown in Fig.2a the fabricated 90μm thick BIT/PZT piezoelectric films can be used as integrated L wave UTs. They can operate in pulse-echo, pitch-catch and transmission configurations. Here only the measurements obtained from the pulse-echo geometry at UT6 is presented. When electric pulses were applied on the piezoelectric film UT through the top and bottom electrodes, where the barrel itself served as the bottom electrode as shown in Fig.2a, ultrasonic waves were excited and transmitted into the barrel in the thickness direction. Figures 2b and 2c show the typical ultrasonic performance of the UT6 with a diameter of 10 mm as shown in Fig.2 in (b) time and (c) frequency domain (of L^1) at 240°C. The 240°C was the highest temperature achieved due to the available hot plate for testing. In Fig.2b the ultrasonic signal shows a signal-to-

noise ratio (SNR) of about 30 dB. The SNR is defined as the ratio of the amplitude of the first echo traveled one round trip through the thickness direction over that of the signals, which are undesired, between the echoes traversing back and forth in the sample. This UT showed a center frequency of 8.6 MHz and had a 6 dB bandwidth of 4.4 MHz. It is noted that BIT/PZT thick film UT has demonstrated a NDT application at temperature more than 400°C [16].

3.2 On Graphite/epoxy Composite Substrate

Graphite/epoxy (Gr/Ep) composites are well used in the transportation and in particular aerospace industry because of their high mechanical strength to weight ratio. To perform in-situ structure health monitoring [17,18] during the use of Gr/Ep composite is highly desired. The highest temperature during the fabrication of a Gr/Ep composite as shown in Fig.3 in the recommended cure cycle was 176°C and the duration was 120 minutes. For such Gr/Ep composite substrate PZT powders in PZT gel was used for film fabrication. During the fabrication, thermal treatment such as drying, firing and heating for corona poling was carried out using a heat-gun producing gentle heat. The furnace and the torch used were proved to be difficult in controlling the heating speed and temperature. In order to not affect the performance of the Gr/Ep composite a thermocouple contacting the surface of the Gr/Ep composite was used to ensure that each heating would not exceed 176°C. It is the intention of this study to evaluate the performance of the PZT/PZT film sensor for thickness measurement under such low temperature thermal treatments. A 70 µm thick PZT/PZT film UT_Z deposited on the flat side and a 90 µm thick PZT/PZT film UT_Y on the center of the cylindrical periphery of a 13.1 mm thick with a radius of 50.8 mm x-y direction cross ply Gr/Ep composite of semi-cylindrical shape shown in Fig.3. The film thicknesses were achieved through applying the process shown in Figure 1 several times where each layer of coating of each film UT proceeded for 20 minutes. The Gr/Ep composite has sufficient conductivity to serve as the bottom electrode for the produced piezoelectric film based UT.

Figures 4a and 4b show a typical ultrasonic performance of the integrated UT_Z with a diameter of 10mm shown in Figure 3 operated in pulse-echo mode at room temperature. In Figure 4a the measured signal-to-noise ratio (SNR) of the ultrasonic signal L^1 is about 11 dB. L^1, L^2, L^3 and L^4 are respectively the 1st, 2nd, 3rd and 4th round-trip reflected echoes through the thickness of the Gr/Ep composite along Z direction. The measured center frequency and 6 dB bandwidth of L^1 is 1.6 MHz and 1.5 MHz, respectively. Figures 5a and 5b show the measured reflected echoes through the thickness of the Gr/Ep composite along Y direction. The measured center frequency and 6 dB bandwidth of L^1 is 1.3 MHz and 0.7 MHz, respectively. By comparing Fig.4a with Fig.5a three distinct differences; pulse duration of the reflected echoes and ultrasonic velocity in the Gr/Ep composite along two different directions were observed. The longer duration of the pulse such as L^1 in Fig.5a than that in Fig.4a was caused by the curvature of the composite shown in Fig.3 which induces different travel time for different part of the film UT. For such a Gr/Ep composite, the thickness along Z and Y direction would be 2.96 mm and 5.10 mm, respectively, per µs time delay in ultrasound for one-way travel at 22°C. It means that the anisotropy exists as expected. The speed of ultrasound is much faster along the cross ply fiber orientation direction than that along the direction perpendicular to the cross ply. The SNR of the ultrasonic signal L^1 in Fig.5a is only 5 dB which is 6 dB

less that that in Fig.4a. It is also learned that the low center frequency in Fig.4b and Fig.5b was caused by the high ultrasonic attenuation within the thick composite. In principle, the ultrasonic attenuation is proportional to the operation frequency squared. The higher frequency components suffer significant higher ultrasonic attenuation.

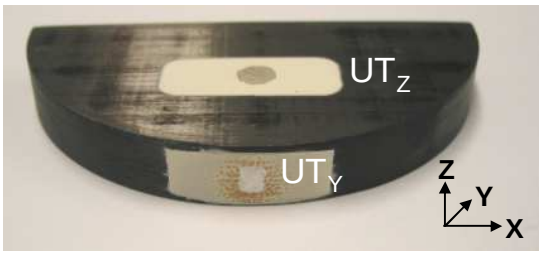

Fig.3. A Gr/Ep composite with 13.1 mm thickness and a radius of 50.8 mm.

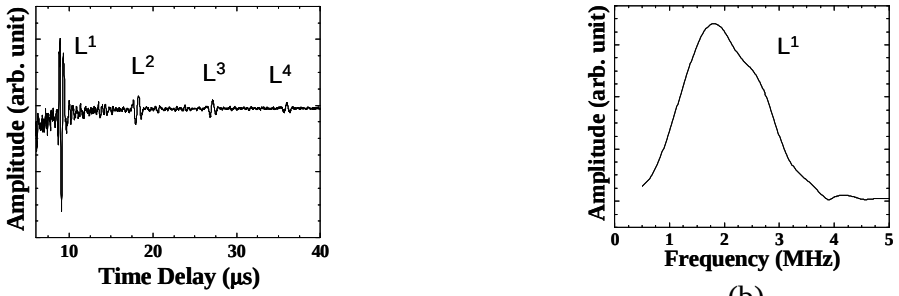

Fig.4. Ultrasonic performance of the UT_Z shown in Fig.3 in (a) time and (b) frequency domain at 22°C.

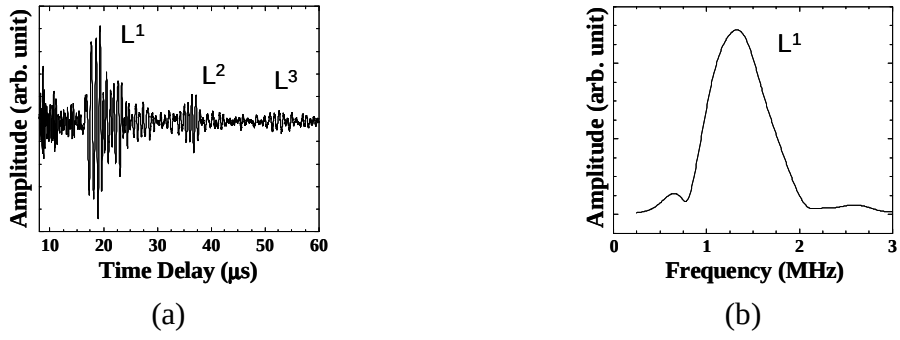

Fig.5. Ultrasonic performance of the UT_Y shown in Fig.3 in (a) time and (b) frequency domain at 22°C.

4. INTEGRATED SHEAR WAVE UTs

4.1 Shear Wave UT

In reference [10,11,17] the mode conversion from longitudinal (L) to shear (S) wave due to reflection at a solid-air interface was reported. It means that the L wave UT together with L-S mode conversion caused by the reflection at a solid-air interface can be effectively used as S wave probe. The L_i wave generated by the L wave UT reaches a

solid-air interface and reflected as L_r and S_r. as shown in Fig.6, where θ is the incident and reflect angle for L wave.

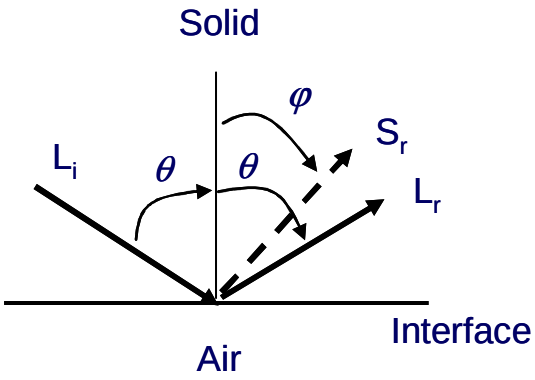

Fig.6 Reflection and mode conversion with an incident longitudinal wave at a solid-air interface.

The equations governing this reflection and mode conversion can be given as [10,11]

$$\frac{V_l}{\sin\theta} = \frac{V_s}{\sin\varphi} \tag{1}$$

$$R_{ll} = \left[\frac{\cos^2 2\varphi - \left(V_s/V_l\right)^2 \cdot \sin 2\theta \cdot \sin 2\varphi}{\cos^2 2\varphi + \left(V_s/V_l\right)^2 \cdot \sin 2\varphi \cdot \sin 2\theta} \right]^2 \tag{2}$$

$$R_{sl} = \frac{4\left(V_s/V_l\right)^2 \cdot \cos^2 2\varphi \cdot \sin 2\theta \cdot \cos 2\varphi}{\left[\cos^2 2\varphi + \left(V_s/V_l\right)^2 \cdot \sin 2\varphi \cdot \sin 2\theta\right]^2} \tag{3}$$

In this study a mild steel with L wave velocity V_l = 5960 m/s and S wave velocity V_s = 3235 m/s was used as the substrate. Figure 7 shows the calculated energy reflection coefficient based on Equations (2) and (3) for the steel sample. It indicates that the maximum energy conversion rate from L and S wave is 97.6% at θ = 67.2° and the reduction of the energy conversion rate is within 1% in the θ range between 60.8° and 72.9°. Our technology considers a simple way to fabricate the L wave UT and let the L UT is in a plane parallel to the mode converted S wave direction as shown in Fig. 8. This approach could reduce the machining and thick film fabrication difficulty and time. By considering this criterion the $\theta + \varphi$ needs to be 90°. From equation (1) which is the

Snell's law we can obtain that θ = 61.5°. At this angle the reduction of energy conversion rate, based on Fig.7, is within 1%. Therefore Figures 8a and 8b show the schematic and actual device for this study. Figures 9a and 9b show the ultrasonic signal in time and frequency domain, respectively, of the received S_r wave in pulse-echo mode at 150°C. The diameter of the L UT was 10 mm. The S^n represents nth round trip of the waves transversing back and forth between the L wave UT and the probing end. The center frequency of the clear S^1 wave was at 5.7 MHz and the 6 dB bandwidth was 4.0 MHz. It can be seen that the received L wave is not visible due to the fact that the length of the substrate has been chosen so that the reflected L waves from the probing end of the probe will not enter into the aperture of the transmitting L wave UT. It is noted that the signal strength of S^1 was 5 dB weaker at 150°C than that at 22°C.

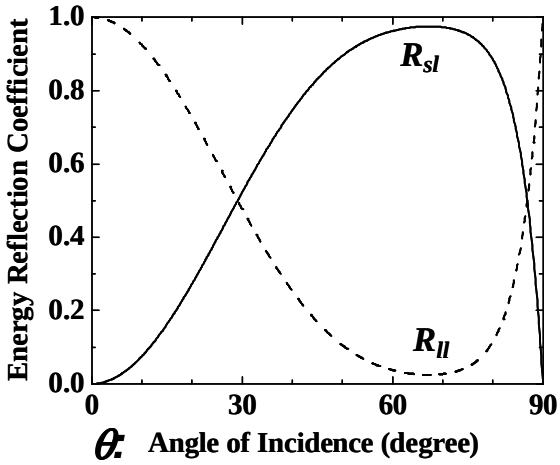

Fig.7 Energy reflection coefficient vs. θ (incident angle)

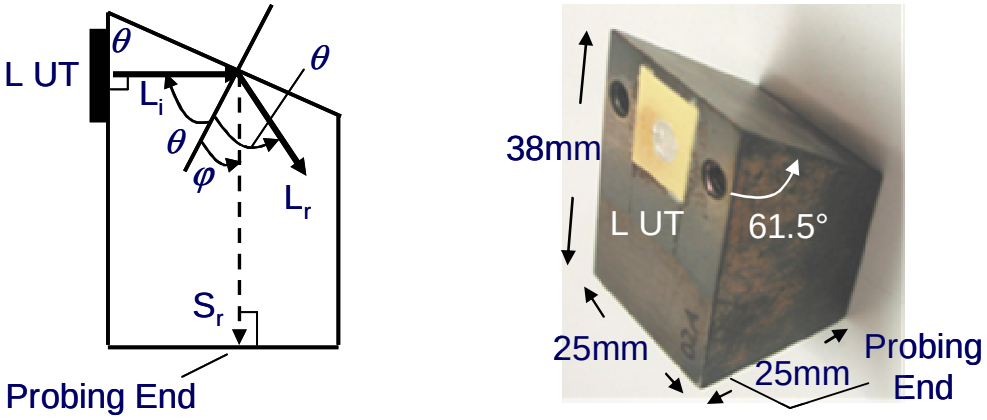

(a) (b)

Fig.8. (a) Schematic diagram and (b) actual device of an integrated S wave UT probe with the L wave UT is located in a plane parallel to the direction of mode converted S wave where θ = 61.5°.

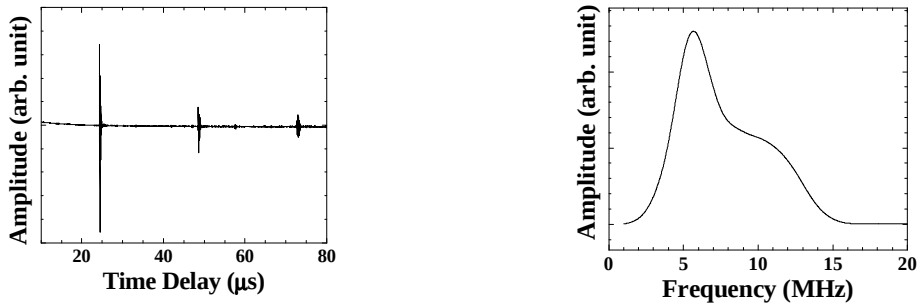

(a) (b)

Fig.9. Ultrasonic signal in (a) time and (b) frequency domain of the S wave UT probe shown in Fig.8 at 150°C. (a)

4.2 Shear and Longitudinal Wave UT Probe

If one would like to use pulse-echo mode to generate and receive both L and S waves, then the UT shown in Fig.8 can be modified to achieve such a purpose. In fact, it simply makes a slanted surface with an angle 45° from the intersection of the slanted plane and the line from the center of the L wave UT as shown in Fig.10. The 45° angle will reflect the energy of the L_i wave into the $L_{r,45°}$ wave. Therefore, in principle, the upper part of the L wave generated from L UT will be used to produce S_r and the lower part to produce the $L_{r,45°}$ wave. Figures 10a and 10b show the schematic and an actual device. Figures 11a, 11b and 11c show the ultrasonic signal in time and frequency domain, respectively, of the received S_r (S^1)and $L_{r,45°}$ (L^1) waves in pulse-echo mode at 150°C. L^1 represents the 1st round trip L wave echo between the L wave UT side and the probing end. The center frequency of the clear S^1 and L^1waves were at 6.2 MHz and 7.3 MHz and the 6 dB bandwidth was 4.0 MHz and 5.9 MHz, respectively. As expected there was no difference in frequency spectra of converted shear waves between Fig.9b and 11b. During the top electrode fabrication for the device shown in Fig.10b the area of top electrode was adjusted so that the amplitude of the reflected S_r and $L_{r,45°}$ waves were nearly the same. It is noted that the signal strength of S^1 and $L^1$was about 5 dB weaker at 150°C than that at 22°C.

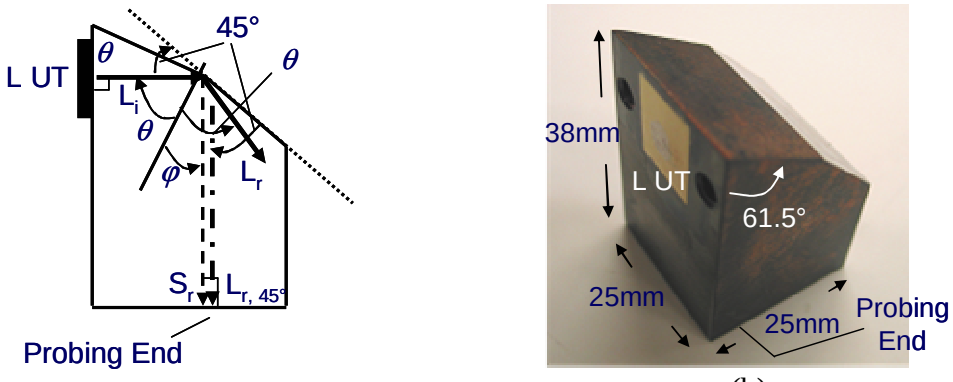

(a) (b)

Fig.10 (a) Schematic diagram and (b) actual device of an integrated L and S wave probe with the L wave UT located in a plane parallel to the direction of S_r wave.

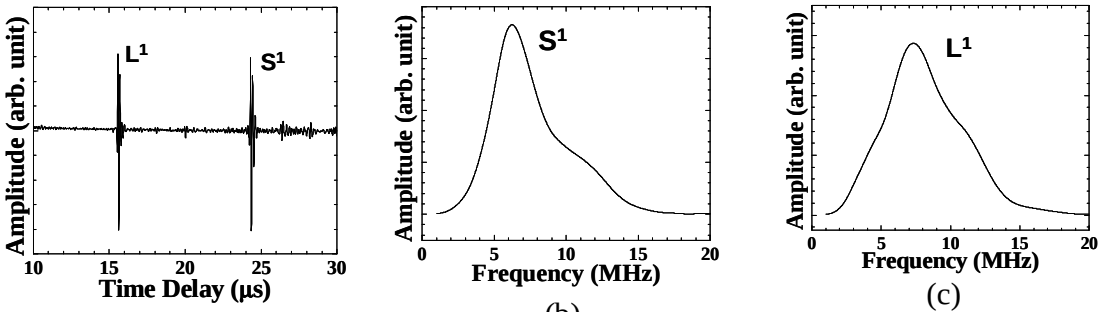

(a) (b) (c)

Fig.11 Ultrasonic signal of the UT in Fig.10 in (a) time and frequency domain of (b) mode converted S wave and the (c) reflected L at 150°C.

5. FLEXIBLE UTs

The same fabrication technique was used to fabricate PZT/PZT or BIT/PZT thick film UTs onto thin metallic membranes [20]. This configuration offers special advantage that the UTs are flexible. The flexibility is realized owing to the porosity of piezoelectric film and the thinness of substrate. Figures 12a and 12b show two views of a PZT/PZT 120μm thick film five UTs array directly fabricated onto a 75μm thick stainless steel membrane with this particular merit. The entire structure was sandwiched by polyimide films except the probing side of the membrane (the side opposite to thick film) so that it can operate with waterproof and at temperatures up to 150°C. Copper strips were used for electrical connections.When this flexible UT array was pressed onto a steel plate of 17.7 mm together with high temperature coupling oil and fixed by a mechanical clamp, the measured ultrasonic signal in time and frequency domain at 150°C are given in Figures 13a and 13b, respectively. It can be seen that the SNR in Figure 13a is 18 dB so that, for instance, the thickness measurement of tube can be accurately performed. The 150°C was limited by the quick evaporation of the coupling oil at high temperature and our mechanical method to attach the flexible transducer to the tube substrate. The center frequency of this transducer is 5.3 MHz. We have also used steel, titanium, nickel and copper membranes for the fabrication of flexible UTs. These flexible UTs with the metallic membranes may be also glued, soldered or brazed or mechanically bound onto cylindrical surfaces for ultrasonic measurements. This flexible UT has been also employed to inspect Gr/Ep composite and polymer materials.

(a) (b)

Fig.12. (a) and (b) A flexible five UT array.

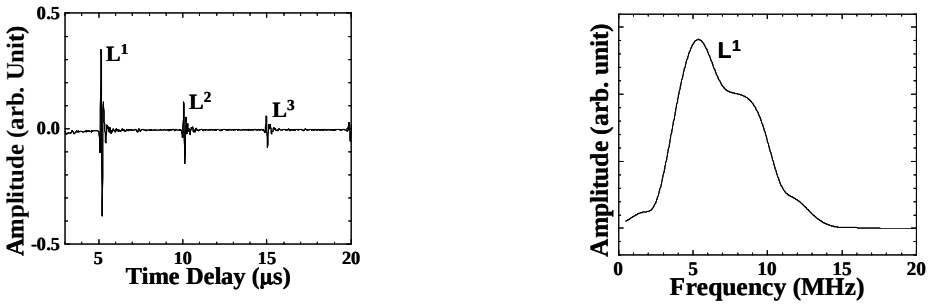

(a) (b)

Fig.13. Ultrasonic signal in (a) time and (b) frequency domain of the flexible UT probe shown in Fig.12 at 150°C. (a)

6. CONCLUSIONS

Thick (> 40μm) PZT/PZT and BIT/PZT ceramic films as piezoelectric ultrasonic transducers (UTs) have been successfully deposited on steel and graphite/epoxy composite substrates by a spray technique. The characteristics of these UTs were that they (1) can be integrated directly onto the desired planar or curved substrates; (2) may not need couplant; (3) can operate in the transmission and pulse/echo modes with a signal to noise ratio more than 30 dB at 2-15 MHz; (4) can operate up to more than 400°C [16]; (5) can be made flexible and (6) can be made as UT array. The thick film was normally used as L wave UT but it has been demonstrated that using the L wave to S wave mode conversion S wave probe and simultaneous S and L wave probe can be made and operated at 150°C. Such films have been also deposited onto 75μm thick stainless steel membranes to form the flexible five-UT array and operated at 150°C.

ACKNOWLEDGMENT

The authors are grateful to Y. Ono, H. Hébert, J.-F. Moisan, K.-T. Wu, Q.-L. Liu and J. Tatibouet for their technical assistance. Financial support from a NRC-NSC, Taiwan project is acknowledged.

REFERENCES

[1] Krautkrämer, J. and Krautkrämer, H., "Ultrasonic Testing of Materials", Springer-Verlag, Berlin, 1990.

[2] Birks, A.S., Green, R.E. Jr. and McIntire, P. ed., "Nondestructive Testing Handbook", 2nd Ed., vol.7: Ultrasonic Testing, ASNT, 1991.

[3] Kundu, T. ed, "Ultrasonic Nondestructive Evaluation: Engineering and Biological Material Characterization", CRC Press, N.Y., 2004.

[4] Lynnworth, L.C., "Ultrasonic Measurements for Process Control", New York: Academic Press, 1989.

[5] Fothergill, J.R., Willis, P. and Waywell, S. "Development of high-temperature ultrasonic transducers for under-sodium viewing applications," British J. Nondestr. Test., vol. 31, pp. 259-264, 1989.

[6] Arakawa, T., Yoshikawa, K., Chiba, S., Muto, K. and Atsuta, Y., "Applications of brazed-type ultrasonic probes for high and low temperatures uses," Nondestr. Test. Eval., vol. 7, pp. 263-72, 1992

[7] Mrasek, A.H., Gohlke, D., Matthies, K. and Neumann, E., "High temperature ultrasonic transducers," NDTnet, vol. 1, no. 9, pp. 1-10, 1996

[8] McNab, A., Kirk, K.J., and Cochran, A., "Ultrasonic transducers for high temperature applications," IEEE Proc. Sci. Meas. Technol., vol. 145, pp. 229-236, 1998.

[9] Karasawa, H., Izumi, M., Suzuki, T., Nagai, S., Tamura, M. and Fujimori, S., "Development of under-sodium three-dimensional visual inspection technique using matrix-arrayed ultrasonic transducer," Journal of Nuclear Science and Technology, vol. 37, pp. 769-779, 2000.

[10] Kobayashi, M., Ono, Y., Jen, C.-K., and Cheng, C.-C., "High temperature ultrasonic transducer and its application to process monitoring of polymer injection molding", IEEE Sensors J. vol.52, pp.55-62, 2004.

[11] Whiteside, B.R., Brown, E.C., Ono, Y., Jen, C.-K., and Coates, P.D. "Real-time ultrasonic diagnosis of polymer degradation and filling incompleteness for micromolding", Plastics, Rubber and Composites: Macromolecular Engineering, vol.34, pp. 387-392, 2005.

[12] Auld, B.A., "Acoustic fields and waves in solids", vol.2, John Wiley & Sons, New York, 1973, pp.30-38.

[13] Mayer, W.G. "Energy partition of ultrasonic waves at flat boundaries" Ultrasonics, 3, pp. 62-69,1965.

[14] Jen, C.-K., Sreenivas, K., and Sayer, M.: 'Ultrasonic transducers for simultaneous generation of longitudinal and shear waves', JASA, 1988, 84, pp.-26-29.

[15] Barrow, D., Petroff, T.E., Tandon, R.P. and Sayer, M. "Characterization of thick lead-zirconate titanate films fabricated using a new sol gel process" J. Apply. Phys., vol.81, pp.876-881, 1997.

[16] Kobayashi, M., and Jen, C.K. "Piezoelectric thick bismuth titanate/PZT composite film transducers for smart NDE of metals", Smart Materials and Structures, vol.13, pp. 951-956, 2004.

[17] Gandhi, M.V. and Thompson, B.S., "Smart Materials and Structures", London; New York, Chapman & Hall, 1992.

[18] Ihn, J.-B. and Chang, F.-K., "Ultrasonic Non-destructive Evaluation for Structure Health Monitoring: Built-in Diagnostics for Hot-spot Monitoring in Metallic and Composite Structures", Chapter 9 in Ultrasonic Nondestructive Evaluation Engineering and Biological Material Characterization, edited by T. Kundu, CRC Press, New York, 2004.

[19] Si-Chaib, M.O., Djelouah, H., and Bocquet, M. "Applications of ultrasonic reflection mode conversion transducers in NDT", NDT&E Int'l, vol.33, pp.91-99, 2000.

[20] Kobayashi, M., Jen, C.K., and Lévesque, D. "Flexible ultrasonic transducers," accepted by IEEE Trans. UFFC, March 2006.